Polymer 51 (2010) 953–958

Contents lists available at ScienceDirect

Polymer

journal homepage: www.elsevier.com/locate/polymer

Swelling and morphological properties of poly(vinyl alcohol) (PVA) and poly(acrylic acid) (PAA) hydrogels in solution with high salt concentration

S.M.M. Quintero [a], R.V. Ponce F [a], M. Cremona [b,*], A.L.C. Triques [c], A.R. d'Almeida [c], A.M.B. Braga [a]

[a] Department of Mechanical Engineering, Pontifícia Universidade Católica do Rio de Janeiro, Rio de Janeiro, Brazil
[b] Department of Physics, Pontifícia Universidade Católica do Rio de Janeiro, Rio de Janeiro, Brazil
[c] CENPES, Petrobras, R.1 Q.7, Cidade Universitária,21949-900 Rio de Janeiro, Brazil

ARTICLE INFO

Article history:
Received 17 August 2009
Received in revised form
10 December 2009
Accepted 13 December 2009
Available online 4 January 2010

Keywords:
Poly(vinyl alcohol)
Poly(acrylic acid)
pH sensor

ABSTRACT

Understanding the swelling properties of hydrogels and how they affect the hydrogel's morphology is of fundamental importance in the development of hydrogel-based artificial muscles, bio-actuators, sensors and other devices. In this paper, the swelling behavior of PVA–PAA hydrogel films in saline water and in buffer solutions of different pH values was investigated. It was observed that the swelling factor of the hydrogel decreases when the ionic strength of the solvent solution increases. Scanning Electron Microscopy (SEM) revealed structures with different pore shapes and sizes depending on the type of solution used for hydration. In saline water, Energy Dispersive X-Ray (EDS) analysis indicated the formation of NaCl crystals within the polymeric network. Finally, the PVA–PAA hydrogel was used as an actuator to strain a fiber Bragg grating sensor, thus providing an indirect measurement of the pH value of the surrounding solution.

1. Introduction

It has been demonstrated that acidic environments, i.e. environments with low pH, increase the corrosion rates of steel and other metallic alloys [1], therefore, causing pitting corrosion in many industrial processing units, such as bleaching and desalination systems, heat exchangers and pipes in petroleum wells [2]. In order to estimate the corrosion rates of devices and equipment in service in acidic environments, it is important to continuously monitor the pH in these environments.

Previously, we have developed a fiber-based pH sensor in which a pH-sensitive hydrogel is coupled to an optical fiber containing a Bragg grating [3,4]. The hydrogel (PVA–PAA) rearranges its network structure according to the pH value and ionic strength of the solution in which it is immersed, converting chemical energy into volume changes that can be explored in different ways. With the aid of an optical fiber with Bragg gratings, the swelling/deswelling of the hydrogel is employed as an actuator to convert changes of the solution's acidity into changes of the optical signal reflected by the gratings. One of the intended applications for this sensor is measuring the pH of fluids in petroleum wells, where other fiber Bragg grating devices are being increasingly employed in real-time monitoring systems for production parameters such as pressure, temperature and flow-rate [5].

As mentioned above, acidity and ionic strength are the critical factors controlling the hydrogel's swelling response and, consequently, the sensitivity of the proposed fiber-based pH sensor. Therefore, it is important to analyze and characterize the hydrogel in saline solutions of different pH values. In this paper, we report and discuss results of experiments carried out to measure the swelling factor of PVA–PAA hydrogel films in solutions with high salt concentration and with different pH values. The response is also correlated with the hydrogel's morphology measured using SEM and Energy Dispersive X-Ray (EDS) analysis. The sensitivity of a fiber-based pH sensor prototype is also reported.

2. Experimental preparation of PVA–PAA hydrogel films, buffer and saline water solutions

Initially, poly(vinyl alcohol) (PVA; average molecular weight, $M_w = 31{,}000$, Aldrich) and poly(acrylic acid) (PAA; average molecular weight, $M_w = 1250.000$, Aldrich) polymers were individually dissolved in ultra pure water at room temperature and at 60 °C, respectively. The two solutions were then mixed together in amounts of equal weight and stirred during one hour at room temperature, in order to obtain a homogeneous solution. Finally, the resulting homogeneous polymer blend solution was poured onto a metallic plate to form a film. The excess water solvent was

* Corresponding author. Tel.: +55 21 35271258 229.
E-mail address: cremona@fis.puc-rio.br (M. Cremona).

0032-3861/$ – see front matter © 2009 Elsevier Ltd. All rights reserved.
doi:10.1016/j.polymer.2009.12.016

further evaporated slowly at 60 °C for 36 h to promote thermal crosslinking of the polymer blend.

When solutions of these polymers are mixed and allowed to evaporate under mild conditions, the esterification reaction between the hydroxyl groups of PVA and the carboxyl groups of PAA brings about the formation of a tridimensional network whose degree of crosslinking depends on conditions of the thermal treatment, such as, temperature, duration and pressure [6–9]. Apart from the insolubility that arises from the thermal evaporation of the mixed solutions (the films are able to swell, but it is not possible to revert them back to the solution state), spectroscopic changes confirm the esterification reaction. Indeed, FTIR spectra (not shown here for the sake of simplicity) of our thermally treated samples demonstrated that, while the C–O stretch mode of the PVA–PAA films (1240 cm^{-1}) is intensified, the peak intensity of the vibration motion of the out of plane O–H (920 cm^{-1}) decreases.

Simultaneously, the carbonyl band at 1730 cm^{-1} increases quantitatively with the crosslinking density of the PVA–PAA films [10,11].

2.1. Saline water and buffer solutions

Saline water was prepared synthetically by weighing the required amounts of salts ($CaCl_2.2H_20$, $MgCl_2.6H_2O$, KCl, $SrCl_26H_2O$, $BaCl_2.2H_20$, NaCl, $NaHCO_3$ and KBr) and distilled water to approximately reproduce the composition of the formation water found in Brazilian oilfields located in Campos Basin [12]. Ionic species and composition of the saline water prepared, whose Ionic Strength was 1.865 M, are listed in Table 1. Several samples with different pH values were prepared. The pH values and ionic strengths of the potassium hydrogen phthalate and potassium phosphate commercial buffer solutions used are shown in Table 2.

2.2. Swelling measurements

Initially, free swell tests were performed in order to characterize the hydrogel swelling response at transient and steady state conditions. In both cases, circular samples (diameter: 7 mm and thickness: 0.25 ± 0.05 mm) were cut from the bulk, dried hydrogel film and weighed. Swelling measurements were conducted using saline water and buffer solution with pH values between 3 and 6. The hydrogel samples were immersed in the solutions at 25 ± 0.5 °C. After hydration, the swollen films were removed from the solution and gently wiped with a tissue to remove any remaining fluid from the surface.

For the transient swelling tests, hydrogel samples initially swollen in buffer solution at pH 3 were rapidly transferred to another beaker with buffer solution at pH 4. The swelling factor (SF) of the hydrogel samples were computed according to Equation (1):

$$SF = \frac{W_f - W_{ref}}{W_{ref}} \times 100\% \quad (1)$$

where W_f is the weight of the hydrated hydrogel in a certain pH and W_{ref} is the weight of the hydrated hydrogel at pH 2.8 (reference pH value). The SF was measured at intervals of 10 min for the first hour and then at intervals of an hour or more, up to approximately 20 h. Equilibrium pH values were obtained from the transient response until no further changes in SF were observed.

Table 1
Ionic species and concentration of the saline water (mg/L).

Na^+	K^+	Ca^{2+}	Mg^{2+}	Sr^{2+}	Ba^{2+}	Cl^-	Br^-
34,000	510	3200	440	570	120	64,055	199

Table 2
pH values and ionic strength of the buffer solutions.

pH	*I* (M)
3.00 ± 0.05	0.2618
4.00 ± 0.05	0.2618
5.00 ± 0.05,	0.0006
6.00 ± 0.05	0.0227

It is important to note that at least three readings in three samples were performed for each swelling measurement.

2.3. SEM and EDS analysis

SEM micrograph analyses were performed in order to investigate the morphology of the PVA–PAA hydrogel films under swollen conditions. Samples hydrated in both synthetic saline water and in buffer solutions at pH 2.8 and pH 5.8, respectively, were fast frozen in liquid nitrogen and then freeze-dried until water sublimation occurred. After drying, the hydrogels were carefully cleaved and their superficial and inner structures were analyzed by using a scanning electron microscope (FEI Quanta 200).

3. Results and discussions

3.1. Swelling measurement in transient condition

Fig. 1 shows the swelling factor variation as a function of the immersion time when the hydrogel sample was moved from a buffer solution at pH 3 to another one at pH 4. The time interval to reach the final volume at pH 4 was of approximately three hours. Since changes in pH in petroleum wells may take weeks, this response time is considered fully satisfactory for the application intended.

3.2. Measurement of the swelling in steady state condition

Fig. 2a and b show the behavior of the swelling factor of the PVA–PAA hydrogel as a function of the pH when in buffer solution (ionic strengths from 0.0006 M to 0.2618 M) and in saline water (ionic strength: 1.865 M), respectively. Comparing both curves, it is clear that the presence of dissolved salts in the saline water – which increase its ionic strength – decreases strongly the swelling of the hydrogel. In fact, within all the pH range investigated, the higher SF found was for samples immersed in the buffer solution with lower ionic strength. The largest SF measured in this solution is more than

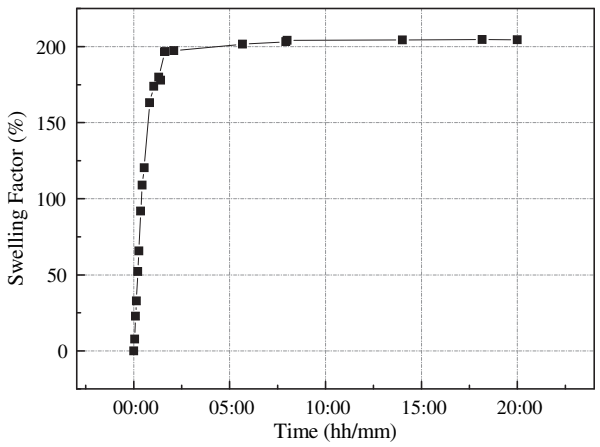

Fig. 1. Transient response of the hydrogel swollen in buffer solution at pH 3 and then transferred to pH 4.

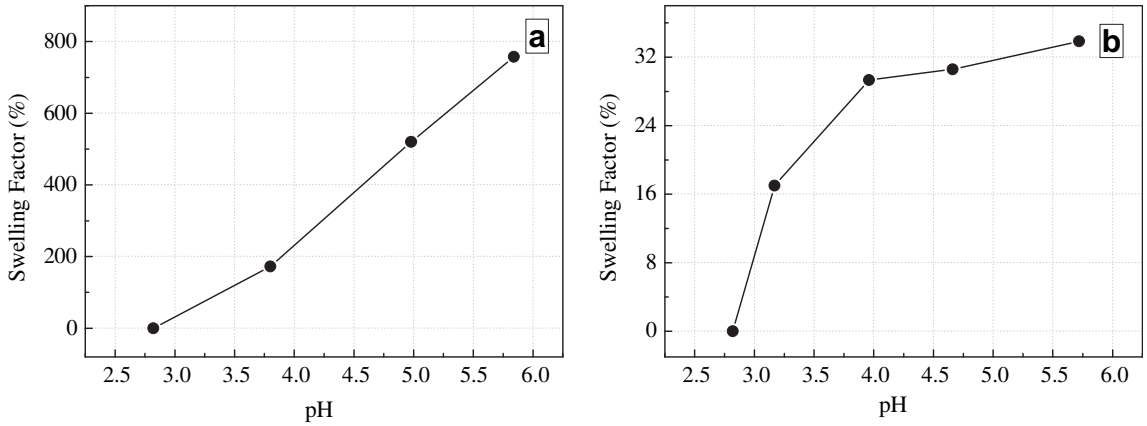

Fig. 2. Swelling factor (SF) of the PVA–PAA hydrogel as a function of pH values in (a) buffer solutions and in (b) saline water.

twenty-two times the SF obtained for the hydrogel film immersed in saline water with the same pH.

Such difference in the hydrogel swelling response can be attributed to solvent absorption and electrochemical interactions, and is ultimately related to the ionic strength of each solution. When the hydrogel is immersed in an aqueous solution, water hydrates the weak acidic carboxylic groups bonded to the PAA polymer. Consequently, at successive pH increments, multiple acid–base equilibrium occurs and the polymer undergoes stepwise swelling as a result of solvent absorption and electrochemical interactions caused by the progressive ionization and neutralization of the –COOH/–COO^- groups [13–15].

Since the buffer solutions have a relatively low ionic strength (see Table 2), there will be absorption of the few mobile ions present in order to balance the osmotic pressure and, consequently, swelling of the polymer. Due to the low ion concentration of the solution located inside the hydrogel, steric interactions among the charged polymer groups will occur, promoting high hydrogel swelling factors such as those observed in Fig. 2a.

In the case of saline water, Fig. 2b the high ionic strength in the solution outside the polymer leads to a higher species diffusion into the hydrogel to balance the osmotic pressure and neutralize the carboxylate groups bonded to the PAA backbone. Consequently, the mobility of the polymer network is strongly reduced by the shielding of the steric effects between the partially ionized carboxylic groups, due to the high content of electrolytes.

This swelling behavior observed is expected when one considers the chemical equilibrium analysis of the hydrogel. Ionization of almost all the carboxylic groups in the PAA backbone occurs at pH values lower than the p*K*a (approximately 4.7) of the polymer [5,16].

3.3. SEM and surface morphology

In Figs. 3 and 4, we present microphotographs obtained for swollen PVA–PAA hydrogel films. Depending on the type of solution used for hydration, samples display significant differences in the porous media morphology.

3.3.1. Samples in buffer solution

As observed in Fig. 3a and b, the internal morphology of swollen and freeze-dried PVA–PAA hydrogel samples hydrated in the buffer solution display irregular pore shapes with variable sizes ranging from 0.2 μm to 1 μm, and open three-dimensional network structures. Fig. 3a displays, in the same SEM microphotograph, the cross-section and the external surface of the hydrogel in buffer solution at the reference pH value of 2.8. One notices that the average pore size close to the edge is always significantly larger than the average pore size observed in the interior region of the hydrogel. The outer surface structure of these hydrogels was slightly flat, but not perfectly smooth, presenting macropores (average size: 2.5 μm) distributed over the entire surface. Fig. 3b shows the cross-section morphology of the hydrogel hydrated in the same buffer solution, but at pH 5.8 (SF = 780%). At higher pH values the hydrogel dramatically expands the structure of the porous network, resulting in larger swelling. Consequently, the pore structure morphology previously observed at the lower pH (Fig. 3a) is completely modified, now exhibiting irregular-sized channels. The drastic

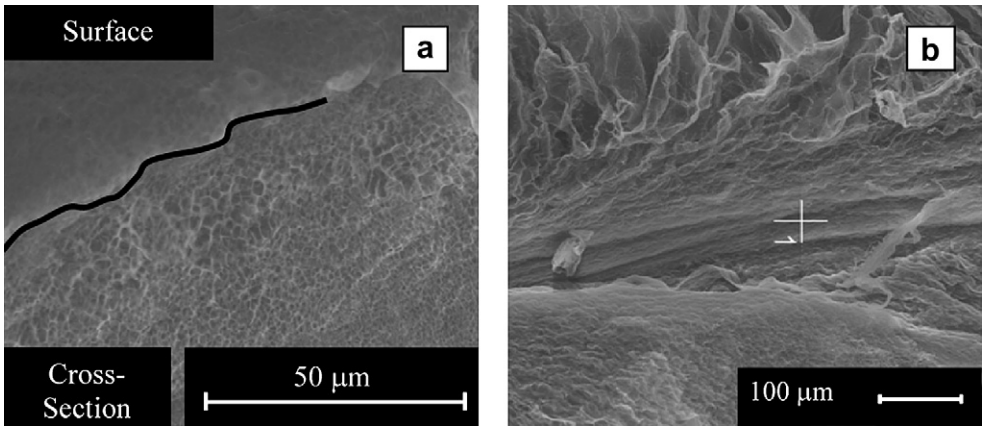

Fig. 3. SEM microphotograph of a freeze-dried PVA–PAA hydrogel immersed in buffer solution for 7 days (a) at pH 2.8 (reference pH value) and (b) at pH 5.8 (SF = 780%).

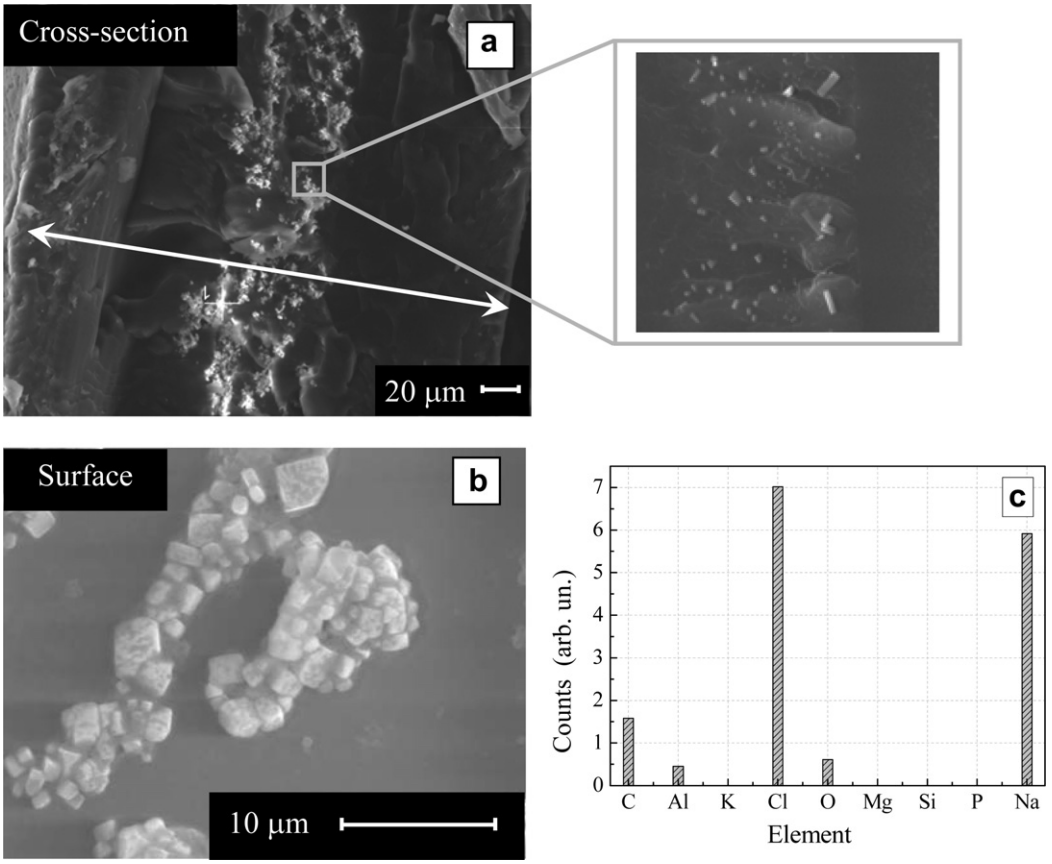

Fig. 4. SEM microphotograph of the freeze-dried PVA–PAA hydrogel previously hydrated in saline water at pH 2.8 for 7 days showing (a) the inner morphology (the inset shows the irregular particles), (b) the outer surface and (c) the EDS spectrum of irregular particles.

differences observed in the pore size and inner structure of hydrogels samples immersed in buffer solutions with pH 2.8 and 5.8 confirms the strong effect of the pH observed in the measured swelling factor.

3.3.2. Samples in saline water

Polymer samples were swelled in saline water at pH 2.8 and 5.8. At pH 2.8, SEM images of the cross-section (Fig. 4a) and surface (Fig. 4b) display the formation of irregular particles deposited inside the hydrogel networks and on the outer surface. The images also confirmed a preferential deposition distribution in a line through the center plane of the hydrogel membrane cross-section. Energy dispersive X-ray spectrometry (EDS) analysis was performed to identify the chemical composition of the solid particles observed in the SEM microphotographs. EDS results in Fig. 4c show the characteristic peaks of the sodium and chlorine ions, indicating the presence of crystals, mostly NaCl, in the solid deposit observed in Fig. 4a and b.

Fig. 5 shows the morphology of the hydrogel swelled in saline water at pH 5.8. Although there is a large amount of crystals, they are not uniformly distributed within the polymeric network. In fact, they are preferentially located along three distinct planes, one in the center and the other two close to the edges. Between the center plane and those close to the edges, the presence of crystals was not observed, and a porous structure is evident by magnifying the image (shown in the inset of Fig. 5). This distribution could be related to crystal precipitations occurring during the rapid sublimation of the hydration solution from the samples.

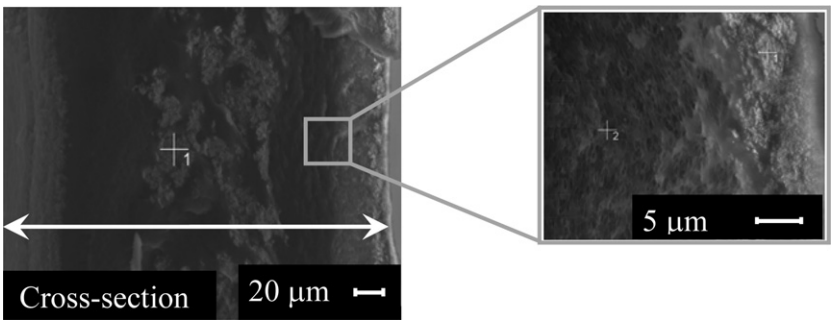

Fig. 5. SEM microphotograph of a freeze-dried PVA–PAA hydrogel immersed in saline water at pH 5.8 for 7 days. The inset shows a magnified section of the image, where the presence of pores between the center line and the lines close to the edges can be seen.

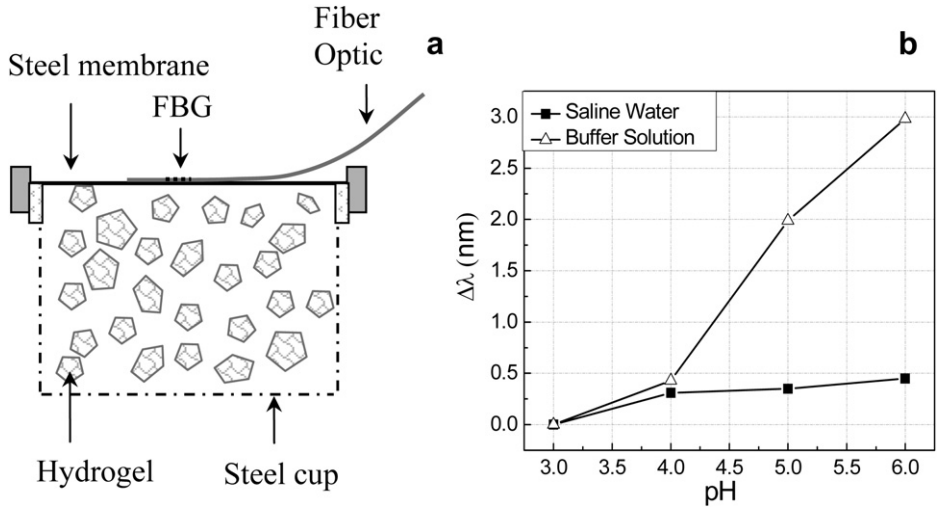

Fig. 6. (a) Side view of fiber grating pH sensor. (b) Experimental shift in the reflected spectrum due to variations of pH.

4. Fiber optic pH sensor

As previously discussed, we have developed a fiber-based pH sensor in which the PVA–PAA hydrogel acts as the actuator [2,3]. The sensor is based on Fiber Bragg Gratings (FBG), which operate as highly selective wavelength filters, reflecting a narrow band of light around its Bragg wavelength. The Bragg wavelength is related to the effective refractive index of the fiber core (n_{eff}) and to the spatial periodicity of the index modulation (Λ) [17]:

$$\lambda_B = 2n_{\text{eff}}\Lambda \tag{2}$$

The basic principle of measuring strains with FBGs lies in monitoring wavelength shifts of the reflected Bragg signal as a function of changes in the effective refractive index or spatial periodicity of the grating. The Bragg wavelength shift due to strain and temperature can be expressed as

$$\Delta\lambda_B = \lambda_B\left[\left(\alpha_f + \zeta_f\right)\Delta T + (1 - p_e)\Delta\varepsilon\right] \tag{3}$$

where α_f is the thermal expansion coefficient of the fiber, ζ_f its thermo-optical coefficient and p_e the optical fiber strain-optical coefficient. In the absence of temperature changes, it is possible to measure strain from the wavelength shift as [17]

$$\varepsilon = \frac{1}{0.77}\frac{\Delta\lambda_B}{\lambda_B} \tag{4}$$

Based on this effect, the sensor employs the hydrogel as an actuator that, in response to changes in pH, strains an optical fiber containing one or more Bragg gratings.

4.1. Design and response of pH sensor

In our fiber-based pH sensor, pieces of hydrogel are placed in a stainless steel cup with permeable walls formed by a rigid mesh (Fig. 6a). The cup is immersed in the solution of which the pH will be measured. This configuration allows rapid diffusive transport, while at the same time preventing the hydrogel to exude through the mesh. When swelling or deswelling, the pieces of hydrogel deform a circular stainless steel membrane clamped along its edge to a rigid metallic house that also supports the permeable cup containing the hydrogel. A FBG is bonded to the membrane, measuring strains imparted to it due to swelling or deswelling of the hydrogel. A side view of the sensor is shown in Fig. 6a.

The sensor response was investigated both in buffer solution and in saline water with different pH values ranging from 3 to 6. According to the results (Fig. 6b), when in buffer solution, the sensor experienced a wavelength shift of approximately 3.0 nm in the full pH range investigated, resulting in a sensitivity of approximately 1 nm per pH unit. This, however, only happens in fluids with low ionic strength, such as the buffer solutions used. In contrast, when immersed in saline water, the sensitivity was much lower, although measurements of pH changes are still feasible in the range pH 3 to 6.

5. Conclusions

In the present work, swelling factors (SF) of hydrogel films were measured in buffer and saline solutions. The SF of hydrogels increased with pH. It was observed, however, that the high concentration of salts dissolved in saline water was responsible for a strong reduction in the swelling factor of the PVA–PAA hydrogel. Such behavior can be credited to the shielding effect of ionic species dissolved in the saline solution. At high ionic strengths, more electrolytes will surround the charged polymeric network, suppressing electrostatic repulsion between the carboxylate groups, hence, reducing the bulk hydrogel SF. Considerable differences in pore sizes and morphologies were observed either in the surface or in the interior of the swollen PVA–PAA hydrogel, depending on the ionic strength of the solution used. In addition, EDS analysis performed on the samples immersed in saline solution indicated the presence of significant amounts of Na and Cl crystals, probably due to crystallization that occurred inside the hydrogel.

The results obtained suggest that PVA–PAA hydrogels are promising candidates to be used in pH sensing, and that they are capable of showing suitable response times and considerable swelling factors in the pH range investigated here. However, for the purpose of indirectly monitoring corrosion, since the swelling factor is strongly reduced in solutions with high ionic strength, it is also necessary to take into account effects of the salt concentration on the swelling response.

Acknowledgements

The authors gratefully acknowledge support from Petrobras and the Brazilian Ministries of Education and Science and Technology, respectively through their agencies CAPES and CNPq. The authors are indebted with Prof. L. Campos Akcelrud for the useful

discussion and help with polymer chemistry. We also thank Dr. L. A. Sena, currently at the Brazilian Institute of Metrology (Inmetro), for his invaluable help with the SEM measurements and Paula M. P. Gouvêa for helping with English text editing.

References

[1] Jangama VR, Srivasan S. Internal report. CLI International Inc; 2003.
[2] Liu CT, Wu JK. Corros Sci 2007;49:2198–209.
[3] Silva Jr MF, D'Almeida AR, Pereira FR, Braga AMB, Triques ALC, Valente LCG. Optical fiber pH sensor. 2006: AR049289.
[4] Triques ALC, Quintero SMM, Veiga HMB, Ferreira MVD, Braga AMB, D'Almeida AR, et al. Optical fiber sensors, OSA technical digest (CD). Optical Society of America; 2006. paper TuE94.
[5] Silva Jr MF, Portella RCM, Izetti RG, Campos SRV. "Technologies trials of Intelligent Field implementation in Carmopolis", Petrobras internal report (SPE 95917).
[6] Jin Xing, Hsieh You-Lo. Polymer 2005;46:5149–60.
[7] Herrera-Kao Wilberth, Aguilar-Vega Manuel. Polym Bull 1999;42:449–56.
[8] Myung David, Koh Wongun, Ko Jungmin, Hu Yin, Carrasco Michael, Noolandi Jaan, et al. Polymer 2007;48:5376–87.
[9] Chun Heung Jae, Lee Sang Bong, Nam Sang Yong, Ryu Soon Hwan, Jung Sun Young, Shin Seung Hoon, et al. J Ind Eng Chem 2005;11(4):556–60.
[10] Park YI, Lee KH. J Ind Eng Chem 1999;5(3):235–9.
[11] Zhang WZ, Satoh M, Komiyama J. J Memb Sci 1987;31(2–3):147–56.
[12] Hernandes R, Melo VLA, Santos JAM, Rosário FF, Bezerra MCM, Rosa KRSA. In: Paper SPE 114112 presented at 2008 SPE International Oilfield Scale Conference held in Aberdeen, UK; 28–29 May 2008.
[13] Ricka J, Tanaka T. Macromolecules 1984;17(12):2916–21.
[14] Flory PJ. Principles of polymer chemistry. Ithaca, NY: Cornell University Press; 1953.
[15] Gehrke SH, Cussler EL. Chem Eng Sci 1989;44(3):559–66.
[16] Greenwald HL, Luskin LS. In: Davidson RL, editor. Handbook of water-soluble gums and resins. New York: McGraw-1E11; 1980. p. 17.1–17.19.
[17] Hill KO, Meltz G. J Lightwave Technol 1997;15:1263–76.